Synthesis and structure of antibacterial coatings formed by electron-beam dispersion of polyvinyl chloride in vacuum

Chun He[a], A.V. Rogachev[a,b], Beibei Li[a], V.A. Yarmolenko[c], A.A. Rogachev[a,b], D.V. Tapal'skii[c], Xiaohong Jiang[a,*], Dongping Sun[a], M.A. Yarmolenko[a,b,**]

[a] International Chinese-Belorussian Scientific laboratory on Vacuum-Plasma Technology, College of Chemical Engineering, Nanjing University of Science and Technology, Nanjing 210094, China
[b] Francisk Skorina Gomel State University, 104, Sovetskaya street, Gomel 246019, Belarus
[c] Gomel State Medical University, 5, Lange street, Gomel 246000, Belarus

ABSTRACT

A new antibacterial coating has been synthesized to modify implants with prolonged release of a medicinal antibacterial component (ciprofloxacin). Condensed in vacuum, the products of electron beam dispersion of PVC were used as one of the components of the target. It is shown that the repeated action of the electron flow on condensed destruction products of PVC is accompanied by the formation of poly-conjugated structures devoid of chlorine. Thermal treatment of the hydrocarbon layer (500 °C) leads to the formation of graphite-like structures and polyene fragments up to 8 units in length. The antibacterial coating (PVC_2-ciprofloxacin) is formed by the action of a low-energy electron flow on a mechanical mixture of ciprofloxacin and condensed PVC destruction products. It is shown that in comparison with the antibacterial layer PU - ciprofloxacin, the proposed coating is characterized by a higher resistance to abrasion. The PU - ciprofloxacin layer is completely worn out after 17 cycles. The worn-out areas of the proposed coating after 17 and 25 wear cycles are 47% and 53% respectively. Heat treatment of the coating, including standard sterilization, does not affect the kinetics of the release of ciprofloxacin from the hydrocarbon matrix. Unlike the PU layer - ciprofloxacin, the prolonged release (sustained release) of ciprofloxacin in PVC_2-ciprofloxacin is not ensured by intermolecular interaction but by the mechanical containment (confinement) of ciprofloxacin using a hydrocarbon matrix. Microbiological studies showed high antibacterial activity of the proposed composite layer in relation to P. aeruginosa and E. coli. The activity was maintained after abrasive coating treatment for 24 h.

1. Introduction

Nosocomial infection is a cause of serious postoperative complications, which in some cases may lead to the death of a patient [1–6]. The control of its consequences requires significant financial costs. Acute infections occur, in prosthetics, when the implants are introduced into the human body.

Currently, the main directions of the fight against bacterial adhesion and the subsequent formation of biofilms on the surfaces of the implants are formulated [1,2,5]. The most effective way of preventing postoperative complications is to use coatings maintaining a prescribed concentration of antibacterial substance near the implant surface for a long time. There are a number of requirements to these coatings, such

as, biocompatibility, self-cleaning, programmable release of the drug component, strong adhesion to the implant surface, resistance to abrasion by soft tissues, etc. The deposition of antibacterial drugs onto a metal implant is not effective, since it may lead to bacterial resistance [5]. This is caused by the inability to maintain the drug concentration above the minimal inhibitory (MIC) for a particular microorganism near the implant surface over a long period of time.

The water-soluble (e.g., PEG) or biodegradable (e.g., polyactide) antibacterial polymeric coatings possess a good self-cleaning function, and can prolong release of the drug component, protect metal nanoparticles from leaching and reduce their cytotoxicity [7]. Physical processing methods, e.g., plasma make it possible to give the polymer coatings the surface energy necessary to stimulate the processes of

tissue regeneration [8]. They make it easy to control the structure and, hence, the kinetics of the release of the drug component. The disadvantage of polymer coating systems is the low wear resistance and weak adhesion with metal surfaces, which probably leads to a rapid loss of coatings during the implant introduction into the body. One should note that all medical devices must undergo the obligatory standard procedure of thermal sterilization before being introduced into the body. This heat treatment may lead to notable structural changes of polymeric coating and thus the properties as well.

Carbon coatings (e.g., DLC) are characterized by high adhesion strength to metal surfaces, wear resistance and biocompatibility [9–11]. Only particles of metals (silver, copper, zinc, etc.) may be act as antimicrobial components of DLC coatings [9–13]. These metals are potentially toxic for cell cultures [1,3,5]. DLC coatings cannot be used as layers with programmable release of the drug component.

Many researchers have pursued various ways to deposit thin layers based on the advantages of carbon and polymer coatings. In particular, one of the methods for preparing such coatings is presented previously [6]. However, this technology cannot be effectively used to modify implants in a wide range of sizes and shapes because of the complexity and multi-stage processes.

The electron-beam polymers dispersion allows the formation of thin antibacterial layers with prolonged release of the drug component [7,14,15]. The plasma pre-treatment of metal substrates provides strong adhesion of coatings with the substrates.

In the work presented, the method of electron-beam formation of antibacterial coatings characterized by high adhesion and wear resistance is proposed. It is suggested to use mix condensed products of electron-beam dispersion of polyvinyl chloride PVC with medicinal compound as a target material. The deposited layer structure is midway between the structure of the polymer hydrocarbon and the DLC layers. Thus, the advantages of both polymer antibacterial layers and carbon layers can be preserved.

2. Methodology of the experiment

2.1. Methodology of forming coatings

The coatings were formed from the active gas phase generated by the action of a low-energy electron beam with 800–1600 eV energy and 0.01–0.03 A/cm^2 density on the target material in a vacuum. The initial pressure of the residual gases in the vacuum chamber was $\approx 4 \cdot 10^{-3}$ Pa.

The composite coatings were deposited from the gas phase formed by the action of electron beam on mechanical mixtures of PVC_1 and ciprofloxacin powders, as well as polyurethane and ciprofloxacin in a 1:1 weight ratio.

It should be noted that it is not possible to obtain a homogenous composite coating using the initial PVC powder. This is due to the fact that the process of electron-beam deposition of a coating, based on PVC, is implemented only after a deep dehydrochlorination of the polymer. This prevents the generation of the gas phase simultaneously containing the destruction products of all the components of the mixture target.

The article deals with the coatings of the same effective thickness. The effective thickness (which was $0.5 \mu m$) of the formed layers was controlled directly during the deposition by means of a quartz thickness gage (QCM).

The substrate temperature at the coatings deposition corresponded to room temperature.

2.2. The material of coatings and substrates

The powder of polyvinyl chloride (Mw ~ 62.000; Mn ~ 35.000; Aldrich), polyurethane (PU, Desmopan 385) and ciprofloxacin (KRKA, Slovenia) was used as a target material.

The material of the coating deposited from volatile products of PVC dispersion (PVC_1) was used as a target subjected to re-electron-beam dispersion for the purpose of producing PVC_2 coatings. The production of PVC_1 was performed in two stages. At the first stage, during the action of the electron flow on the PVC powder, a coating on glass substrates was deposited. At the second stage, the formed layer was scraped off.

The substrates for deposition of the coatings based on PVC_2 were quartz plates (obtaining UV–Vis spectra), NaCl plates (IR spectroscopy studies), silicon (100) single crystal plates (XPS studies), titanium plates $50 \times 50 \times 0.5$ mm (antibacterial studies, wear resistance studies), aluminum plates Ø 5 mm (antibacterial studies).

2.3. Features of the heat treatment of the formed coatings

The coatings were heat-treated in vacuum (10 Pa) and in air at $120\,°C$, $220\,°C$ temperature for 60 and 120 min. Some coatings were annealed in vacuum at $500\,°C$ for 120 min. The temperature range $(120 \div 220)\,°C$ is used for thermal sterilization of medical devices, implants in particular. Heat treatment at a pressure of < 10 Pa is not possible. Heating the coating in high vacuum conditions is accompanied by decomposition of a thin layer and its transition to the gas phase.

2.4. Structure and morphology studies

The thermogravimetric analysis was carried out with DTG-60 (Shimadzu) under nitrogen atmosphere. The heating rate was $10\,°C/$min. The mass of the test material was 3 mg.

The molecular structure of the coatings was investigated on Vertex-70 (Bruker) using a standard transmission thermocell. PVC_1 was analyzed using the method of multiple frustrated total internal reflection (MFTIR). The scanning was performed in the range of 4000–500 cm^{-1} with a resolution of 4 cm^{-1}. A band of stretching vibrations of C−H bonds in CH_2 groups (2920 cm^{-1}) was taken as an internal standard band. The optical density of the band 2920 cm^{-1} linearly depends on the layer thickness. The values of the optical densities of the analyzed bands were correlated with the absorbance of the internal standard band. The degree of oxidation of a thin layer was assessed in relation to the band of stretching vibrations of carbonyl groups C=O (1730 cm^{-1}) [16].

The UV–Vis spectroscopic studies were performed using a Cary-50 (Varian) spectrophotometer using a standard transmission thermocell.

The chemical composition of the deposited layers was determined by the XPS method. The measurements were done on a PHI Quantera II Scanning XPS Microprobe spectrometer using an Al Kα source of monochromatic X-rays (hν = 1486.6 eV). The analysis results were processed using the OriginPro software package.

2.5. Microbiological studies

The antibacterial activity of the coatings was studied for the following microorganisms:

Pseudomonas aeruginosa ATCC 27853–0.5 μg/ml minimum inhibitory concentration (MIC) of ciprofloxacin 0.5 μg/ml (certified value);

Escherichia coli ATCC 25922–0.008 μg/ml minimum inhibitory concentration (MIC) of ciprofloxacin (certified value).

Initially, the titanium plates with a deposited coating were placed in cylindrical containers (80 mm diameter), coatings up, with addition of 35 g of glass beads (3 mm diameter) and 100 ml of bidistilled water (Fig. 1). The containers were incubated in Biosan ES-20 orbital shaker-incubator at 35 °C and 120 rpm for 1, 4 and 24 h. After treatment, each sample was rinsed with distilled water and sterilized by air: 160 °C temperature, 60 min. At the second stage, the sterile titanium plate was placed, coating up, in a Petri dish containing 20 ml of frozen Müller-Hinton agar (MHA). 18 ml of melted and cooled down to 45 °C MHA was poured by a pipette dispenser onto the plate surface as a second
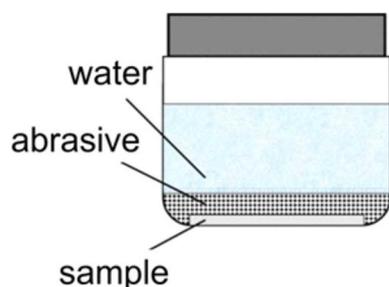
Fig. 1. Scheme of washing samples with a deposited coating before microbiological studies.

layer (the calculated height of the MHA layer above the plate surface is 2 mm, the volume of MHA above the plate surface is 5 cm^3) and held at room temperature until the complete solidification of the medium. After that, the cups were dried with a partially opened lid for 15 min at 35 °C. From the daily cultures of *P. aeruginosa* ATCC 27853 and *E. coli* ATCC 25922, grown on a dense nutrient medium (Nutrient agar, Hi-Media), bacterial suspensions with 0.5 McFarland absorbance were prepared in a sterile isotonic sodium chloride solution. The dishes with the plates were divided into 2 equal sectors with a marker, the suspensions of *P. aeruginosa* ATCC 27853 and *E. coli* ATCC 25922 were applied with a tampon (one in each sector) onto the surface of the second MHA layer. The dishes were incubated for 18 h at 35 °C, after which the presence and nature of the microorganisms' growth were evaluated in the projection of the plates.)

2.6. Kinetics of ciprofloxacin release out of the coating

The kinetic features of ciprofloxacin leaching from the composite layer were established by placing quartz substrates (1.5 × 0.5 cm) with the deposited coating in an isotonic aqueous NaCl solution (0.9%, 100 ml). The substrates placed into the solution were kept in a thermostat at a temperature of 36.6 °C. Before measurement, the solution was vigorously shaken for 1 min. Then the substrates were removed and dropped into distilled water. The drying was carried out in a stream of warm dry air. A change in the absorbance of the ciprofloxacin band was recorded with the spectrophotometer. The kinetics features of ciprofloxacin release from the composite layers based on PVC$_2$ and polyurethane were comparatively analyzed. Particular attention was paid to the study of the effect of preliminary heat treatment of coatings on their ability to prolong the release of ciprofloxacin.

2.7. Study of the wear resistance of coatings

The abrasion resistance of the formed coatings was evaluated using a reciprocating tribometer. The load is 60 g, the length of the abraded area is 17 mm. The indenter was a steel ball (5 mm diameter), on which two layers of calico were fastened. Before attrition, the indenter was wetted in a 0.9% aqueous solution of sodium chloride (NaCl). This test pattern simulated the case of interaction of the coating with soft tissues of a body. After abrasion, the samples were scanned. The area of worn-out portions was analyzed using ImageJ software. The number of complete abrasion cycles (17 and 25) was selected based on preliminary studies, taking into consideration the features of the software package.

3. Results and discussion

3.1. Results of differential scanning calorimetry

Two periods of intensive mass loss were observed in thermogravimetric curves of PVC powder in Fig. 2. At the indicated time intervals, the processes of dehydrochlorination and the subsequent thermal destruction of the formed conjugated system take place [17–19]. The initial noticeable decrease in polymer mass was observed near 300 °C, with the subsequent one near 450 °C. The thermogravimetric curve of the condensed products of PVC electron-beam decomposition lacks the areas of intensive mass loss. Heating is accompanied by a smooth change in the mass of the sample. The change in the weight of the sample becomes noticeable at a temperature just slightly above 200 °C.

On the DTA curve of the PVC$_1$ there are no pronounced endothermic peaks. Meanwhile, the endothermic peaks for the initial PVC powder are the most pronounced. The presence of two peaks is due to a two-stage character of the polymer thermal decomposition. The heating of the PVC$_1$ is followed by the appearance of a noticeable exothermic peak near 110 °C and a number of weakly pronounced exothermic bands ranging from 110 to 500° C. The blurriness of exothermic bands may be caused by endothermic decompositions. The total heat balance is shifted toward exothermic processes. The described character of the thermally initiated reactions causes the convex appearance of the DTA curve (Fig. 2b). It should be noted that the presence of exothermic bands in the range of 310–365 °C is characteristic for the PVC powder as well. The exothermic reactions are the result of the chemical interaction of unsaturated bonds with the formation of a cross-linked structure. For PVC, such reactions are only possible after the dehydrochlorination. The cross-linking reactions increase the heat resistance of the organic layer. So, for the PVC powder in the temperature range of 365–435 °C the mass change of the sample is not fixed.

Based on the calorimetric studies, a number of preliminary conclusions may be drawn: 1) dehydrochlorination reactions are not peculiar to PVC$_1$; 2) heat treatment of the destruction products initiates exothermic processes of their cross-linking. The latter conclusion is obvious and confirmed by a large number of publications on dehydrochlorination reactions of PVC.

3.2. Results of IR spectroscopy studies

In the wave number range of 20,000–4000 cm^{-1}, there are two absorptive peaks at 18,500 cm^{-1} and 15,500 cm^{-1} correlated with the absorption in *cis*-(CH)$_x$ and *trans*-(CH)$_x$ unsaturated regions respectively (Fig. 3) [20]. For PVC$_1$ powder, the absorbance at 18,500 cm^{-1} is the most pronounced as compared to that of a PVC$_2$ thin layer. There are a number of other bands (dotted lines in the spectrum), which cannot be unambiguously correlated with the absorption of polyene fragments of linear macromolecules. The presence of these bands in the IR spectrum indicates the interaction of unsaturated fragments with each other (cyclization, cross-linking reactions).

The IR spectrum of PVC$_1$ exhibits high-intensity absorption at 700 and 740 cm^{-1}. In the absence of a band at 700 cm^{-1}, the absorption at 740 cm^{-1} may be due solely to the absorption of C–H out-of-plane in *cis* [20]. The simultaneous appearance of the two absorption bands in the IR spectrum is an indicator of the presence of aromatic fragments in the organic compound. According to Bellamy's data [16], the absorption at 700 and 740 cm^{-1} is due to out-of-plane deformation vibrations of C–H bonds in monosubstituted benzene compounds. The conjugation of double bonds with benzene rings is manifested by absorption near 3030 cm^{-1} and 1600 cm^{-1} [16]. In the PVC$_1$ spectrum there is absorption near 3019 and 3050 cm^{-1}, which is probably ascribed to the vibrations of C–H groups in the *trans* and *cis* regions, respectively [20]. The absorption at 1590 cm^{-1} indicates the presence of aromatic rings. The absorption at 814 cm^{-1} is attributed to *cis* C–H out-of-plane deformation vibrations, while the absorption at 940, 965 and 1020 cm^{-1} results from *trans* C–H out-of-plane deformation vibrations. The presence of low-intensity absorption bands at 630 and 607 cm^{-1} (C–Cl) in the IR spectrum indicates the incomplete original PVC dehydrochlorination process [16].

In the IR spectrum of PVC$_2$, all the absorption bands noted for PVC$_1$ are present in the wave number range of (4000–600) cm^{-1}. Meanwhile, the absorption at 740 and 700 cm^{-1} is not the most intensive, but pronounced enough. A qualitative difference of the IR spectrum of the
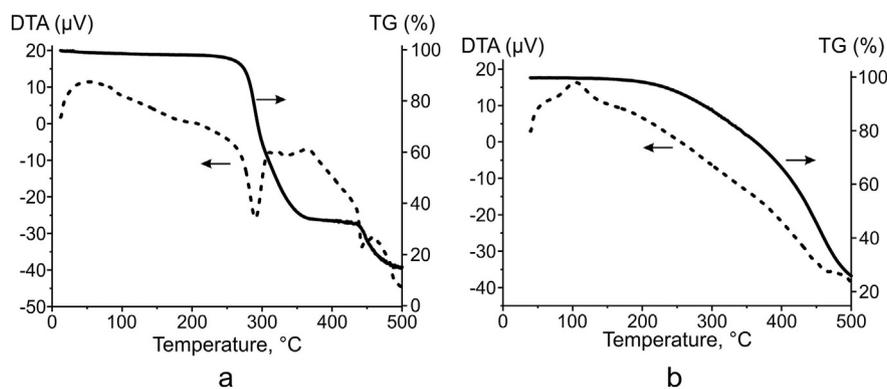
Fig. 2. Results of thermal studies: a – PVC powder; b – the powder of condensed products of electron-beam PVC decomposition (PVC₁).

PVC2 from the spectrum of the PVC₁ is the absence of absorption bands of C—Cl bonds, as expected.

One should note that the method of electron-beam dispersion makes it impossible to form coatings based on high-molecular compounds with aromatic structures (polystyrene, polyethylene terephthalate, etc.). The aromatic fragments are easily detached from the chemical compounds by the electron beam and removed by a vacuum pumping system. The formation of aromatic structures is thereupon implemented only directly on the substrate.

The heat treatment of the coatings in vacuum and in air leads to a decrease of unsaturated bonds (absorbance at 3019 and 3050 cm^{-1}) (Table 1). This decrease becomes more pronounced when the annealing temperature rises. The quantitative determination of the temperature influence on the aromatic fragments is difficult. The decrease in the absorbance at 3019–3050 cm^{-1}, and the decrease in the overall unsaturation level, may also be associated with the decrease in the content

Table 1
Results of IR spectroscopy studies.

Material and treatment type	Wave number, cm^{-1}					
	3019	3050	989	965	940	814
PVC₁	0.154	0.118	0.093	0.159	0.176	0.546
PVC₁ + annealing 500 °C (1 h)	0.103	0.098	0.056	0.051	0.114	0.198
PVC₁ + annealing 500 °C (2 h)	0.426	0.531	0.104		0.382	1.693
PVC₂	0.147	0.134		0.025	0.017	0.089
PVC₂ + annealing 120 °C	0.132[a]	0.132		0.032	0.024	0.104
	0.140	0129		0.016	0.011	0.052
PVC₂ + annealing 220 °C	0.095	0.115		=	–	=
	0.116	0.113		0.011		0.025

[a] Numerator: the results obtained at annealing in air; denominator: in vacuum.
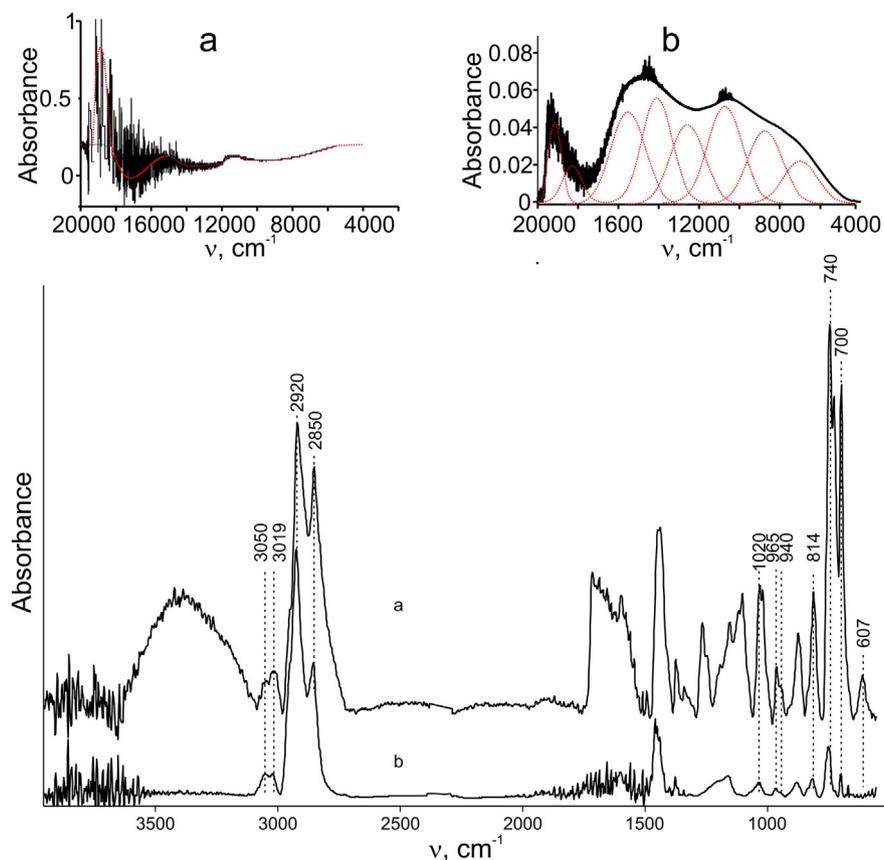
Fig. 3. Results of IR studies of PVC₁ (a) and PVC₂ (b).

Table 2
The impact of annealing parameters on D_{1730}/D_{2920} value.

Coating	D_{1730}/D_{2920} (C = O/CH$_2$)
PVC$_2$	0.026
PVC$_2$ + annealing 120 °C (1 h)	0.107/0.041
PVC$_2$ + annealing 220 °C (1 h)	2.122/0.060
PVC$_2$ + annealing 500 °C (2 h)	− /1.110

Note – in air/in vacuum.

of aromatic structures.

It should be noted that the temperature influences may promote unsaturated bonds occurrence. This is illustrated by the example of high-temperature heat treatment (500 °C) of PVC$_1$. In this case, the growth of unsaturation is caused by the decomposition of the hydrocarbon molecules, which is consistent with the results of thermal analysis and the theory of thermal cracking of hydrocarbons.

Heat treatment of PVC$_2$ initiates the interaction of double unsaturated bonds with each other and air oxygen exerts a noticeable effect on the ratio of carbonyl to CH$_2$ groups (Table 2). A consequence of such interactions at temperatures up to 200 °C is a decrease in the overall unsaturation level and the appearance of carbonyl groups.

3.3. Electron spectroscopy

Linear polyenes have a strong electronic absorption band that shifts to the long-wavelength region with increasing conjugated double bonds [18]. The polyenes containing no > 7 conjugated C=C bonds have absorptive capacity in the UV region, and polyenes with a longer chain (n ≥ 8) – in the visible region [21].

The electronic spectrum of PVC$_2$ has a pronounced absorption band at 267 nm (Fig. 4), which may be related to the length of the polyene fragment [21]. It is worth noting that the assignment of individual maxima in the electronic spectrum of PVC to polyenes of certain length is rather approximate. In particular, it is necessary to take into consideration that *trans*-isomers absorb at longer wavelengths than *cis*-isomers [21]. According to the IR spectroscopy, both *trans*- and *cis*-isomers exist in the deposited hydrocarbon coatings.

In the electronic spectra of heat-treated PVC$_2$ coatings, the
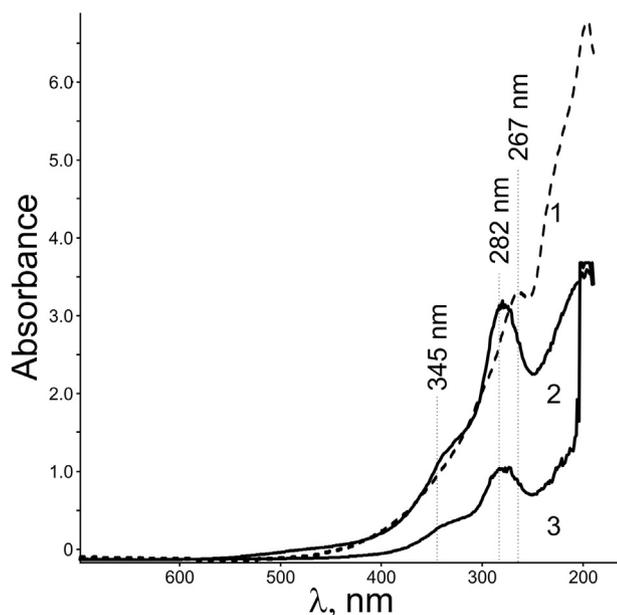
absorption band shifts from 267 nm to 282 nm, together with an absorption at 345 nm. The heating initiates the formation of extended polyene fragments with a length of up to 8 units. We note that the annealing medium has no significant effects on the position of the absorption bands.

3.4. XPS studies

The chemical composition of the formed PVC$_2$ layers was studied by decomposition of the C1s band into individual peaks (Fig. 5). The bands at 282.6, 283.5, 284.3 and 285.1 eV correspond respectively to the C−Si bond [22], the sp^1 hybridized state of carbon atoms, C−C (sp^2 hybridization)/C−H bonds, and C−C (sp^3), C−H bonds [23,24]. The bands corresponding to the absorption of aromatic rings coincide with the individual bands of this set [25]. A high content of sp-carbon atoms (69–82%), observed in XPS results, indicates that the formed PVC$_2$ coatings are poly-conjugated structures. Low-temperature treatment reduces the proportion of sp-carbon atoms, and also increases the proportion of sp^2-carbon atoms. Thus, thermally initiated interactions of double bonds with one another are followed by the formation of graphite structures. This is in full agreement with the IR spectroscopy results (Table 1).

Thin coatings are susceptible to oxidation in air without additional thermal initiation. O1s spectrum of a thin layer can be decomposed into three bands: 532.5, 531.3 and 530.1 eV due to C−O, C=O and the oxidation of the graphite component of a thin layer [26–28]. The heat treatment leads to a redistribution of a thin near-surface layer of oxygen-containing groups, so that the amount of carbonyl groups decreases with increasing annealing temperature. The occurrence of C=O groups is accompanied by a destruction of the main carbon chain of the coating. In addition, low-molecular compounds can easily be evacuated by a vacuum system. It is noticeable that C−Cl bonds were not detected in the coatings by XPS technology.

3.5. AFM studies

The PVC$_2$ coatings are characterized by developed morphology (Fig. 6). Developed morphology can contribute to the mechanical fixation and retention of the antibacterial component on the layer surface.

3.6. Kinetic features of drug component release

Fig. 7 shows the kinetic features of the ciprofloxacin release from composite coatings. It should be noted that the coating of ciprofloxacin is completely dissolved in aqueous medium.

The curve of the kinetic dependence of the ciprofloxacin release from the composite layer has two linear sections. The relatively fast period of ciprofloxacin release (the first 330 min) gives way to a slower one. Similar feature was revealed previously [7]. PVC$_2$ organic matrix promotes a continuous and relatively even release of ciprofloxacin from the composite layer. The composite polyurethane layer is not characterized by such a smoothed release of ciprofloxacin. This difference is due to the low amount of polar groups in PVC$_2$. The emergence of a strong intermolecular interaction between the polyurethane and ciprofloxacin is the main contribution to the abrupt changes in the concentration of drug in the thin layer. Strong intermolecular interaction prevents not only the uniform release of the antibacterial component, but also its subsequent transition to an isotonic solution (biological medium). The surface layer of the coating can easily absorb the molecules of the drug component. Gradual swelling and subsequent destruction of the polyurethane layer in the aqueous medium is accompanied by a formation of new surfaces. This reduces the uniformity of the ciprofloxacin release.

The annealing of composite coatings, as a rule, results in a significant decrease in optical absorbance of ciprofloxacin in IR spectrum.

Fig. 4. Effect of heat treatment (200 °C) of the coatings based on PVC$_2$ on their electronic spectra: 1 – without heat treatment; 2 – heat treatment in air; 3 – heat treatment in vacuum.
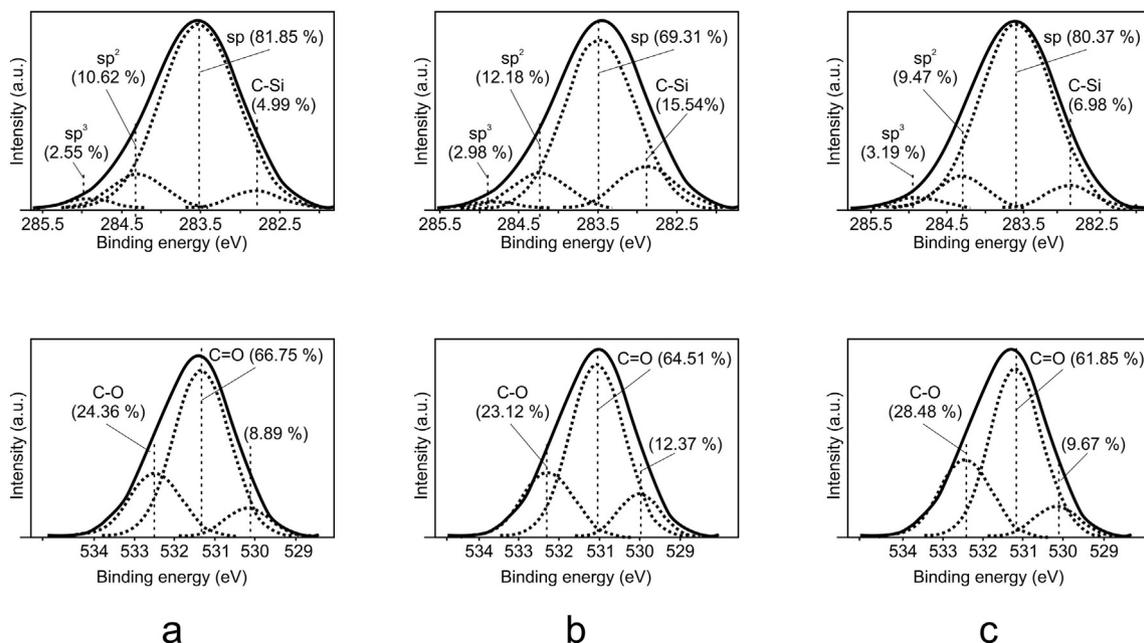
Fig. 5. XPS of PVC$_2$ (a), PVC$_2$ annealed in vacuum for 2 h at 220 °C (b), 500 °C (c).
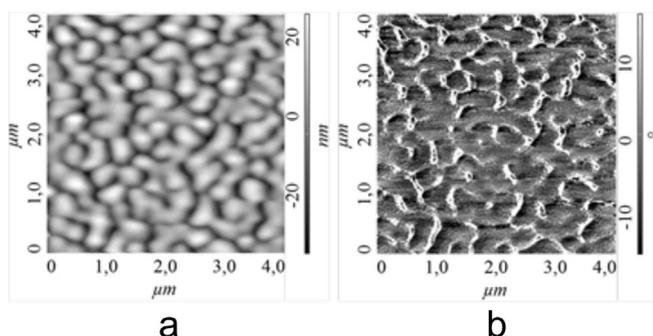
Fig. 6. AFM image of PVC$_2$ coating: a – topography mode; b – phase contrast.

Thus, low-temperature treatment, as the process of medical sterilization, is capable of initiating the destruction of the organic matrix, which has not been taken into consideration in most published scientific papers. The annealing medium of the PVC$_2$ coating, unlike the PU coating, does not influence the kinetic features of ciprofloxacin release. Heat treatment of thin layers helps smoothing the kinetic curves of ciprofloxacin release. This is caused by the influence of heat treatment on the structure of the coating. It should be noted that the release of ciprofloxacin from the heat-treated PU layers occurs step-like. This limits the use of such coatings to maintain a predetermined concentration of the antibacterial component near the surface of the implant.

3.7. Microbiological studies

The results of microbiological studies of PVC$_2$ – ciprofloxacin coatings are shown in Fig. 8.

The coating, that was not abrasive-treated, suppressed the growth of both reference strains in the medium in the projection of the plate and away from it (5 mm for *P. aeruginosa* and at least 12 mm for *E. coli*). The differences in the size of the growth inhibition zones are explained by the different sensitivity of the control strains to ciprofloxacin (MIC of ciprofloxacin 0.5 μg/ml for *P. aeruginosa* and 0.008 μg/ml for *E. coli*).

The abrasive treatment resulted in the decrease of the ciprofloxacin concentration in the coating, which was manifested by the decrease in the size of the growth inhibition zone of *E. coli* around the plate, which is down to 7 mm after 4-hour treatment and 5 mm after 24-hour
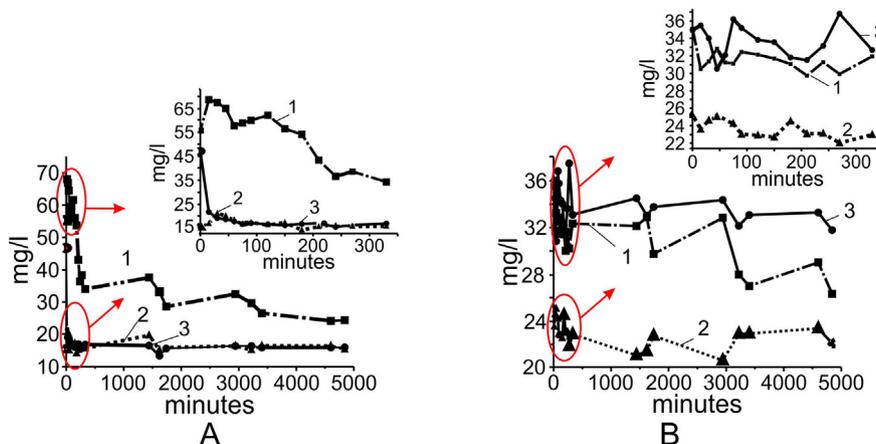
Fig. 7. Kinetics of change in ciprofloxacin concentration in the coatings of PVC$_2$ – ciprofloxacin (A) and PU – ciprofloxacin (B) after prolonged exposure to isotonic solution: 1 – without heat treatment; 2 – annealing in air; 3 – annealing in vacuum.
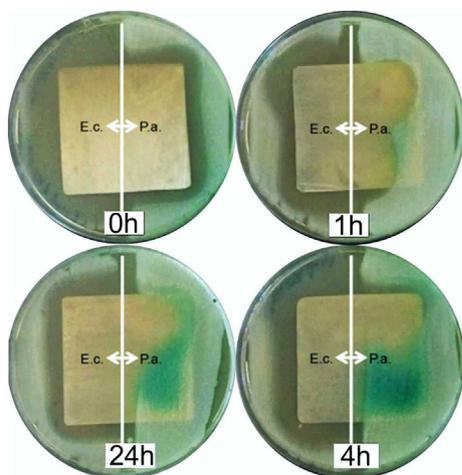
Fig. 8. Bactericidal activity of coatings before and after abrasive treatment against *E. coli* ATCC 25922 (E.c.) and *P. aeruginosa* ATCC 27853 (P.a.).
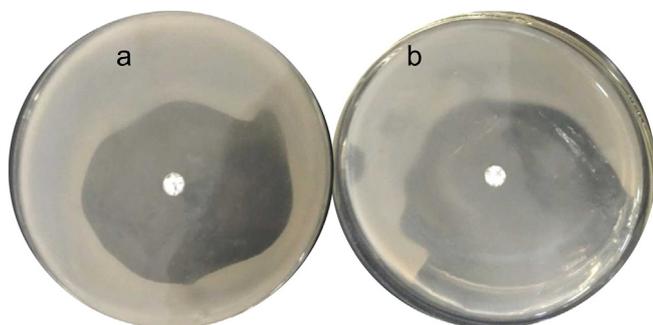
Fig. 9. The zones of growth inhibition of *Staphylococcus aureus* by coatings PU – ciprofloxacin (a) and PVC$_2$ – ciprofloxacin (b) (annealing in air. 220 °C, 1 h).

treatment.

The concentration of the antibiotic after 24-hour abrasive treatment was insufficient to inhibit the growth of *P. aeruginosa* on the medium surface in the projection of the plate. Thus, taking into account the MIC values of the control strains and the volume of the nutrient medium under the plates' surfaces (distribution volume), the release of ciprofloxacin was > 0.1 μg/cm^2 for the initial coating, and from 0.0016 to 0.1 μg/cm^2 for the coatings subjected to abrasive treatment of various durations.

The zones of growth inhibition of microorganisms by coatings PVC$_2$ – ciprofloxacin and PU – ciprofloxacin are presented in Fig. 9. The concentration of the antibiotic in the coatings is the same. The inhibition zone of *Staphylococcus aureus* growth on PU – ciprofloxacin coating is less pronounced than on the PVC$_2$ – ciprofloxacin. The result confirms earlier conclusions about the influence of intermolecular interaction on the kinetics of ciprofloxacin release.

3.8. Features of coatings abrasion

The PVC$_2$ coating is characterized by an increased resistance to abrasion as compared to a thin layer on PU. Thus, after 17 and 25 wear cycles of the polyurethane layer, the area of worn-out areas (without coating) is 8.5% and 21% of the total area of the friction path. A thin PVC$_2$ layer did not wear out under similar wear cycles modes. Composite coatings exhibit significantly lower wear resistance as compared to single-component layers. The PU – ciprofloxacin layer is completely worn out after 17 cycles. The worn-out areas of the PVC$_2$ – ciprofloxacin coating after 17 and 25 wear cycles are 47% and 53%, respectively. The use of PVC$_2$ matrix significantly increases wear resistance of the antibacterial layer.

4. Conclusions

Electron-beam exposure to PVC initiates dehydrochlorination processes. Condensed in a vacuum, the products of PVC destruction contain practically no chlorine. The repeated action of electron flow on the condensed dispersion products is followed by a poly-conjugated structure formation, which is completely free of chlorine.

Heat treatment of a coating based on PVC$_2$ initiates the exothermic interaction processes of double unsaturated bonds. The consequence of these interactions is the formation of graphite-like structures and polyene fragments with a length of up to 8 units. The impact of the temperature may manifest itself not only in reducing the content of unsaturated bonds, but it also may promote their occurrence. This process takes place under conditions of high-temperature heat treatment (500 °C). In this case, the growth of unsaturation is caused by destruction of the hydrocarbon layer.

Continuous heat treatment in the air is followed by a noticeable oxidation of the hydrocarbon coating.

The PVC$_2$ – ciprofloxacin layers, as compared with similar PU – ciprofloxacin layers, are characterized by a much more even release of the drug component into aqueous media. They have a higher resistance to abrasion as well.

The annealing medium PVC$_2$, unlike the coating based on PU, does not affect the kinetic features of ciprofloxacin release. Heat treatment of thin layers helps to smooth the kinetic curves of ciprofloxacin release.

Coatings based on PVC$_2$ may be effectively used to form antibacterial layers with prolonged release of the drug component on the implants surfaces.

Acknowledgement

References

[1] C.L. Romanò, S. Scarponi, E. Gallazzi, D. Romanò, L. Drago, Antibacterial coating of implants in orthopaedics and trauma: a classification proposal in an evolving panorama, JOSR. 10 (2015) 157.

[2] M. Cloutier, D. Mantovani, F. Rosei, Antibacterial coatings: challenges, perspectives, and opportunities, Trends Biotechnol. 33 (2015) 637–652.

[3] C. Nie, Y. Yang, C. Cheng, L. Ma, J. Deng, L. Wang, C. Zhao, Bioinspired and biocompatible carbon nanotube-Ag nanohybrid coatings for robust antibacterial applications, Acta Biomater. 51 (2017) 479–494.

[4] M. Cloutier, R. Tolouei, O. Lesage, L. Lévesque, S. Turgeon, M. Tatoulian, D. Mantovani, On the long term antibacterial features of silver-doped diamond like carbon coatings deposited via a hybrid plasma process, Biointerphases 9 (2014) 029013.

[5] J. Grischke, J. Eberhard, M. Stiesch, Antimicrobial dental implant functionalization strategies – a systematic review, Dent. Mater. J. 35 (2016) 545–558.

[6] S. Buchegger, C. Vogel, R. Herrmann, B. Stritzker, Antibacterial metal ion release from diamond-like carbon modified surfaces for novel multifunctional implant materials, JMR. 31 (2016) 2571–2577.

[7] Qi Chen, A.V. Rogachev, D.V. Tapal'skii, M.A. Yarmolenko, A.A. Rogachev, Xiaohong Jiang, E.V. Koshanskaya, A.S. Vorontsov, Nanocomposite coatings for implants protection from microbial colonization: formation features, structure, and properties, Surf. Coat. Technol. 315 (2017) 350–358.

[8] S. Najeeb, Z. Khurshid, J.P. Matinlinna, F. Siddiqui, M.Z. Nassani, K. Baroudi, Nanomodified peek dental implants: bioactive composites and surface modification – a review, Int. J. Dent. 2015 (2015) 381759.

[9] O.V. Penkov, V.E. Pukha, S.L. Starikova, M. Khadem, V.V. Starikov, M.V. Maleev, D.-E. Kim, Highly wear-resistant and biocompatible carbon nanocomposite coatings for dental implants, Biomaterials 102 (2016) 130–136.

[10] M. Cardoso, J. Sangalli, C.Y. Koga-Ito, L.L. Ferreira, A.S. da Silva Sobrinho, L. Jr Nogueira, Coating with diamond-like carbon films to reduce implant-abutment bacterial leakage, J. Periodontol. 87 (2016) 168–174.

[11] T.T. Liao, T.F. Zhang, S.S. Li, Q.Y. Deng, B.J. Wu, Y.Z. Zhang, Y.J. Zhou, Y.B. Guo, Y.X. Leng, N. Huang, Biological responses of diamond-like carbon (DLC) films with different structures in biomedical application, Mater. Sci. Eng. C Mater. Biol. Appl. 69 (2016) 751–759.

[12] M. Cloutier, S. Turgeon, Y. Busby, M. Tatoulian, J.J. Pireaux, D. Mantovani, Controlled distribution and clustering of silver in Ag-DLC nanocomposite coatings

using a hybrid plasma approach, ACS Appl. Mater. Interfaces 8 (2016), https://doi.org/10.1021/acsami.6b06614.

[13] S.N. Robertson, D. Gibson, W.G. MacKay, S. Reid, C. Williams, R. Birney, Investigation of the antimicrobial properties of modified multilayer diamond-like carbon coatings on 316 stainless steel, Surf. Coat. Technol. 314 (2017) 72–78.

[14] A. Rogachev, M. Yarmolenko, A. Rogachou, D. Tapalski, Xiaoheng Liu, D. Gorbachev, Morphology and structure of antibacterial nanocomposite organic-polymer and metal-polymer coatings deposited from active gas phase, RSC Adv. 3 (2013) 11226–11233.

[15] Sun Jinguo, A.V. Rogachev, M.A. Yarmolenko, A.A. Rogachev, Xiaohong Jiang, D.V. Tapal'skii, D.L. Gorbachev, A.A. Bespal'ko, Nanocomposite coatings based on copper and the products of polyethylene destruction, features of their formation, structure and antibacterial properties, RSC Adv. 6 (2016) 29220–29228.

[16] L.J. Bellamy, The Infra-red Spectra of Complex Molecules. Molecular Spectra, Methuen, Methuen & Co. Ltd., London, 1954, p. 323.

[17] A. Jiménez, V. Berenguer, J. López, A. Sánchez, Thermal degradation study of poly (vinyl chloride): kinetic analysis of thermogravimetric data, J. Appl. Polym. Sci. 50 (1993) 1565–1573.

[18] V.V. Krongauz, Yann-Per Lee, A. Bourassa, Kinetics of thermal degradation of poly (vinyl chloride) thermogravimetry and spectroscopy, J. Therm. Anal. Calorim. 106 (2011) 139–149.

[19] R.R. Stromberg, S. Straus, B.G. Achhammer, Thermal decomposition of poly(vinyl chloride), J. Polym. Sci. 35 (1959) 355–368.

[20] H. Fujimoto, K. Kamiya, J. Tanaka, Optical constants of polyacetylene, Synth. Met. 10 (1985) 367–375.

[21] K.S. Minsker, E.O. Krats, On attributing maximums in electron adsorption spectra of dehydrochlorinated polyvinylchloride and the calculation of polyene sequence distribution, VMS. 13 (1971) 1205–1207.

[22] J. Hackley, D. Ali, J. DiPasquale, J.D. Demaree, C.J.K. Richardson, Graphitic carbon growth on Si(111) using solid source molecular beam epitaxy, Appl. Phys. Lett. 95 (2009) 133114.

[23] M. Rybachuk, J.M. Bell, Electronic states of trans-polyacetylene, poly(p-phenylene vinylene) and sp-hybridised carbon species in amorphous hydrogenated carbon probed by resonant Raman scattering, Carbon 47 (2009) 2481–2490.

[24] A. Hu, M. Rybachuk, Q.-B. Lu, W.W. Duley, Direct synthesis of sp-bonded carbon chains on graphite surface by femtosecond laser irradiation, Appl. Phys. Lett. 91 (2007) 131906.

[25] J.L. Solomon, R.J. Madix, Orientation and absolute coverage of benzene, aniline, and phenol on Ag (110) determined by NEXAFS and XPS, Surf. Sci. 255 (1991) 12–30.

[26] L. Lai, L. Chen, D. Zhan, L. Sun, J. Liu, S.H. Lim, C.K. Poh, Z. Shen, J. Lin, One-step synthesis of NH_2-graphene from in situ graphene-oxide reduction and its improved electrochemical properties, Carbon 49 (2011) 3250–3257.

[27] S.V. Tkachev, E.Yu. Buslaeva, A.V. Naumkin, S.L. Kotova, I.V. Laure, S.P. Gubin, Reduced graphene oxide, Neorganicheskie Materialy. 48 (2012) 909–991.

[28] M. Lu, H. Cheng, Y. Yang, A comparison of solid electrolyte interphase (SEI) on the artificial graphite anode of the aged and cycled commercial lithium ion cells, Electrochim. Acta 53 (2008) 3539–3546.